

The final publication is available at IOS Press through <https://doi.org/10.3233/FAIA190167>. Access to this work was provided by the University of Maryland, Baltimore County (UMBC) ScholarWorks@UMBC digital repository on the Maryland Shared Open Access (MD-SOAR) platform.

Please provide feedback

Please support the ScholarWorks@UMBC repository by emailing scholarworks-group@umbc.edu and telling us what having access to this work means to you and why it's important to you. Thank you.

Iterative Optimization of Orbital Dynamics Based on Model Prediction

Yuhao Hu^{a,c}, Gang Li^b, and Aimin Hu^c

a. School of Astronautics, Harbin Institute of Technology, Harbin 150000, PR China

b. Department of Mechanical Engineering, University of Maryland, Baltimore County, Baltimore, MD 21250, USA

c. Zhenjiang Epsilon Electronics Co., Ltd., Zhenjiang 212000, PR China

Abstract: Aiming at the problem of damage caused by the resonance of chuck and roller in sliding guideway of vehicle. The three-dimensional force and smoothness of sliding mechanism are studied. An improved guideway system is designed in the grey model. In the non-linear optimization design [1], the trust domain multi-objective optimization algorithm is used to divide the model into a series of sub-regions. The model is solved iteratively in the trust region of the sub-region, and the design parameters satisfying the requirements of the smoothness of the guideway are obtained. In ADAMS, the oblique vibration and force motion of components are simulated and analyzed when the track system is running normally. In this paper, the load and amplitude of the roller of sliding guide are studied. An optimization example of sliding guide is given. The results show that the force acting on each group of guide roller mechanism can be effectively decomposed by using the multi-roller design with separated forces. The smoothness and reliability of the system are improved.

Key words: Sliding guide; Multi-body dynamics; Sub-force; Trust Region

0. Preface

Sliding door is an important part of business and heavy load transportation, widely used in business cars, passenger cars and high-speed EMUs and other types of vehicles. Sliding guide is the most critical components of the sliding door. Compared with the traditional revolving door, the sliding door opens large, occupy small space, and is hard to collision, etc. With a signal control, hydraulically driven sliding guide has been gradually developed into a new type of rolling supporting rail. With small friction, high positioning precision and convenient [2], lubrication is becoming a direction of the precise development of vehicle parts in the future, but the structure is complex and the manufacturing precision is more difficult.

Today, domestic and foreign scholars have studied the design [3], vibration noise and applications of the sliding door, and kinetic analysis of the non-automotive sliding rail. Whereas, there is no vehicle rail dynamic simulation research yet. [4] In this paper, a new type of sliding guide design is proposed, which effectively differentiates the stress of the conventional model components with stress concentration and obtains a better regularity simulation results.

1. Establishment of the Gray Model of Sliding Guide under Restricted Space

1.1 Analysis of Existing Sliding Guide Model

At present, the actual use of sliding rails includes two types: two sets of rails matching the single-wheel fixed pulley and three sets of rails matching the directional-strained roller. The load capacity

of one-wheel fixed-sliding system for each guide is limited, and the bending part of the roller is easy to get stuck when sliding to the track or when passing through rails, the roller is easy to wear through as a great friction is produced under the external force, so that the system is low reliability and a shorter service life. Compared to the first type of rail, engineers design the system of three sets of rails matching the directional-strained rollers to work in more conditions. In this system, each set of rollers equipped with the positioning wheels for guiding and the load wheels for specialized loading bearing. The roller of this system has a clear division of labor, and to ensure that the load-bearing wheel will not be hit by other side-force than the stress surface of the rail due to the location change. The bearing wheel only works from the vertical direction of the door, while the rotation of the sliding door is entirely guided by the guide wheel.

1.2 Prediction of Dynamic Model Based on MATLAB

Taking the middle guide as an example, the roller mechanism is divided into positioning wheel and guide wheel, and the vibration is transmitted to the rotating work-piece (component 3) and support arm (component 4) by positioning wheel (component 1) and guide wheel (component 2) on the ground of the guide. A five-degree-of-freedom vibration model of the sliding wheel system of the middle guide is established.

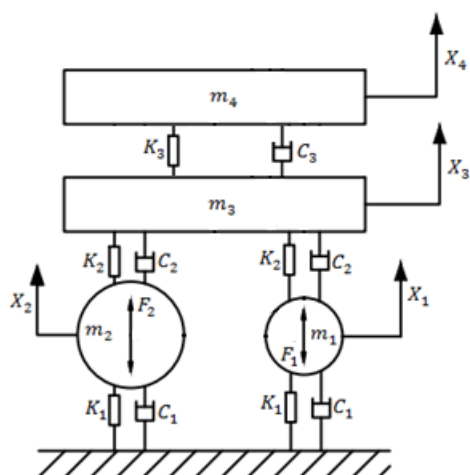


Fig 1 Structural sketch of system dynamics

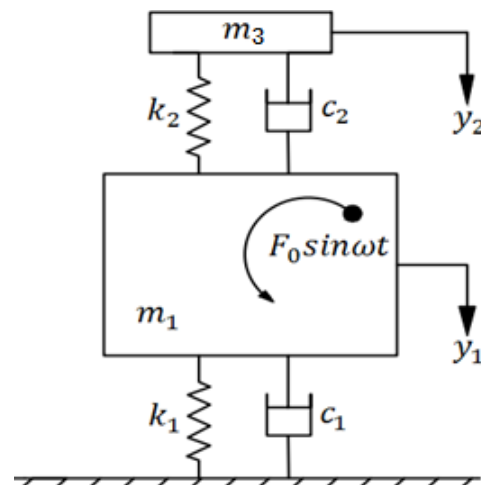


Fig 2 Structural sketch of guide wheel vibration

In fig 1, K_1 is the equivalent stiffness of rotating work-piece, K_2 is the equivalent stiffness of roller, K_3 is equivalent stiffness of guideway, C_1 is the rotating work-piece damping, C_2 is the equivalent damping of roller, C_3 is the equivalent damping of guideway, m_1 is the quality of guide wheel, m_2 is the quality of positioning wheel, m_3 is the quality of rotating work-piece, m_4 is the quality of support arm, x_1 is the displacement of guide wheel, x_2 is the displacement of positioning wheel, x_3 is the displacement of rotating work-piece, x_4 is the displacement of support arm, F_1 is the excitation force of guide wheel, F_2 is the exciting force of positioning wheel.

The work done by calculating the kinetic energy, potential energy and non-conservative force of the system is expressed as

$$T = \frac{1}{2} m_1 \dot{x}_1^2 + \frac{1}{2} m_2 \dot{x}_2^2 + \frac{1}{2} m_3 \dot{x}_3^2 + \frac{1}{2} m_4 \dot{x}_4^2 \quad (1)$$

$$V = \frac{1}{2} k_1 x_1^2 + \frac{1}{2} k_1 x_2^2 + \frac{1}{2} k_2 (x_1 - x_3)^2 + \frac{1}{2} k_2 (x_2 - x_3)^2 + \frac{1}{2} k_3 (x_4 - x_3)^2 \quad (2)$$

$$\delta_w = \sum_1^5 Q_i \delta_i = -c_1 \dot{x}_1 \delta x_1 - c_1 \dot{x}_2 \delta x_2 - c_2 (\dot{x}_1 - \dot{x}_3) \delta (x_1 - x_3) - c_2 (\dot{x}_2 - \dot{x}_3) \delta (x_2 - x_3) + F_1 \delta x_1 + F_2 \delta x_2 \quad (3)$$

According to Lagrange equation $\frac{d}{dt} \left(\frac{\partial T}{\partial \dot{q}_i} \right) - \frac{\partial T}{\partial q_i} + \frac{\partial V}{\partial q_i} + \frac{\partial \phi}{\partial q_i} = Q_i$ ($i = 1, 2, \dots, n$), by sorting out the generalized coordinate x_1 、 x_2 、 x_3 、 x_4 , the kinematic differential equation of the vibration system is obtained as follows:

$$m_1 \ddot{x}_1 + (c_1 + c_2) \dot{x}_1 - c_2 \dot{x}_3 + (k_1 + k_2)x_1 - k_2 x_3 = F_1 \quad (4)$$

$$m_2 \ddot{x}_2 + (c_1 + c_2) \dot{x}_1 - c_2 \dot{x}_3 + (k_1 + k_2)x_2 - k_2 x_3 = F_2 \quad (5)$$

$$m_3 \ddot{x}_3 - c_2 \dot{x}_1 - c_2 \dot{x}_2 + (2c_2 + c_3) \dot{x}_3 - c_3 x_4 - k_2 x_1 - k_2 x_2 + (2k_2 + k_3)x_3 - k_3 x_4 = 0 \quad (6)$$

$$m_4 \ddot{x}_4 - c_3 \dot{x}_3 + c_3 \dot{x}_4 - k_3 x_3 + k_3 x_4 = 0 \quad (7)$$

Formula 4-7 is a five-degree-of-freedom differential equation system with coupling terms, so it is necessary to analyze the whole system step by step in dynamic response analysis, using MATLAB simulation. A two-degree-of-freedom dynamic model (Fig 2) is established by taking the vibration of the guide wheel of the middle guide as an example.

Firstly, the dynamic mathematical model of the system is deduced and the differential equation of motion is established.

$$m_1 \ddot{y}_1 + k_1 y_1 - k_2 (y_2 - y_1) = F(t) - c_1 \dot{y}_1 - c_2 (\dot{y}_1 - \dot{y}_2) \quad (8)$$

$$m_1 \ddot{y}_1 + k_2 (y_2 - y_1) = -c_2 (\dot{y}_2 - \dot{y}_1) \quad (9)$$

$$F(t) = F_0 \sin \omega t = M e \omega^2 \sin \omega t \quad (10)$$

Taking displacement and velocity as state variables

$$\dot{x}_1 = x_2 \quad (11)$$

$$\dot{x}_2 = [M e \omega^2 \sin \omega t - (k_1 + k_2)x_1 - (c_1 + c_2)x_2 + k_2 x_3 + c_2 x_4] / m_1 \quad (12)$$

$$\dot{x}_3 = x_4 \quad (13)$$

$$\dot{x}_4 = [k_2 y_1 + c_2 x_2 - k_2 x_3 - c_2 x_4] / m_3 \quad (14)$$

Drawing displacement response (Fig 3) curves of y_1 、 y_2 with MATLAB and F_s of vibration on guide(Fig 4)

$$F_s = \sqrt{(k_2 x_2)^2 + (c_2 \dot{x}_2)^2} \quad (15)$$

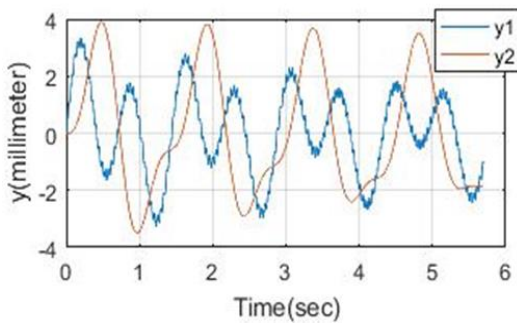


Fig 3 System Displacement Response

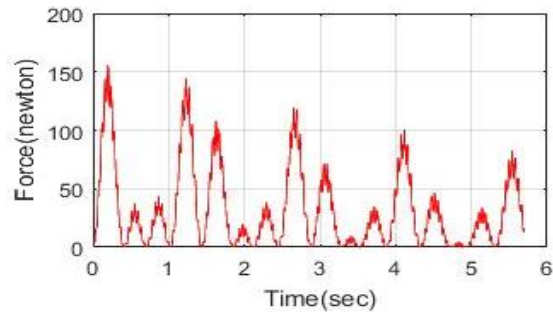


Fig 4 The force of the vibration wheel on the ground

It can be seen from the figure that the vibration and force of the roller have a downward trend. But the peak force is too large, which will cause wear and tear of the guide. The reliability of the whole system is greatly reduced. Therefore, it is necessary to optimize the guide.

2. Optimization Design of Rail Based on Trust Region Iteration Algorithm

2.1 Multi-objective Optimization Algorithm for Gray Model Based on Trust Region

Multi-objective Optimization Algorithm for Trust Region Model [6] is used to solve the nonlinear optimization problem by all-around [7-9]. Using the approximate model to arrange points and to achieve the results by iterative convergence.

The multi-objective optimization algorithm for Grey Model based on trust region divides the complex nonlinear design space into a series of subspace (Trust Region) rather than establishing a surrogate model in the whole design space [10-11]. The trust region is continuously updated by optimizing the trust field in the process of optimization and through the approximate solution on the trust region to ensure that the non-dominated solution would be obtained in line with the real model. The guide in the Grey Model is used to structure the subspace and the iterative algorithm of the trust region to optimize approximately. The uniform distribution solution is verified from the results of approximate optimization. The verified non-dominated solution set verifies the interval of the scaling and translation of the next trust region, and stores each region range in the external solution set, which is continuously expanded with the increase of the number of iterations.

2.2 Algorithm construction and process

In practical engineering problems, the constraint function that satisfies the optimization goal is unknown, and the target model is usually evolved through the Grey Model [12-13]. The multi-objective optimization algorithm of the gray scale model of the trust region is transformed into the solution on the subspace of the trust region. The interval value generated by each iteration is the base domain of the next calculus [14-15] until the convergence criterion is reached.

Generally, the all-around multi-objective nonlinear optimization problem can be described as follows [16]:

$$\text{Minimize} \quad \tilde{f}(X) \quad (16)$$

$$\text{Subjected to} \quad \tilde{g}_i(x) \geq 0, \quad i = 1, \dots, P \quad (17)$$

$$\tilde{h}_j(X) = 0, \quad j = 1, \dots, q \quad (18)$$

$$\max[X_l, X_l^{(k)}] \leq X \leq \min[X_u^{(k)}, X_u], \quad X = [x_1, \dots, x_n] \quad (19)$$

The above codes, $\tilde{f}(x)$, $\tilde{g}(x)$ and $\tilde{h}(x)$ respectively identify and design the surrogate models of the objective function, inequality and equation constraints functions. X_l and X_u respectively represent the upper and lower bounds of the design variable. $X_l^{(k)}$ and $X_u^{(k)}$ respectively represent the upper and lower bounds of the design variable in the NO.K trust region.

The prediction through the model verify the contraction and amplification of the trust region, and the location of the layout point determines the trust center point. If approaching the target model, the trust region will be enlarged otherwise contracted. The trustworthiness $\rho^{(k)}$ [17] is used to verify the optimization with the comparison between the current Grey Model and the target model. The passed value updates the next region of the trust region [18]. The trustworthiness is defined as follows [19]:

$$\rho^{(k)} = \frac{f(X^{(k)}) - f(X^{(k)*})}{\tilde{f}(X^{(k)}) - \tilde{f}(X^{(k)*})} \quad (20)$$

The optimal approximate solution $X^{(k)*}$ is obtained in the current trust region. The trustworthiness $\rho^{(k)}$ is expressed in the design point $X^{(k)}$ and $X^{(k)*}$, the ratio of the actual target function to the

change of the gray model predicted. The closer $\rho^{(k)}$ to 1, the closer between the Grey Model and the target model in the current trust region.

2.3 Iterative optimization of bending part of the guide

The optimization problem of rails can be transformed into the problem between the bending length and the distance under the limited force. Free vertical distance is the display expression; you can build the optimization model [20].

$$\begin{aligned} & \text{Min } \{f, F\} \\ & f = \frac{pL^3}{48EI_z} = \frac{5000}{\frac{1}{12}x_3(x_1-2x_4)^3 + \frac{1}{6}x_2x_4^3 + 2x_2x_4\left(\frac{x_1-x_4}{2}\right)^2} \\ & \text{S.t } F=245\sqrt{2}\sin(x_i - x_j) \end{aligned} \quad (21)$$

In this, f is the free-end vertical distance of guide, F is the lateral wall of the guideway force, f and F are the nonlinear functions of x_i . x_i and x_j are the length of the bending part of the guideway. $x_0 = 0$, $0 < x_1 < 50$, $50 \leq x_2 < 100$, $100 \leq x_3 < 150$, $150 \leq x_4 < 200$. $i=0, 1, 2, 3$, $j=i+1$.

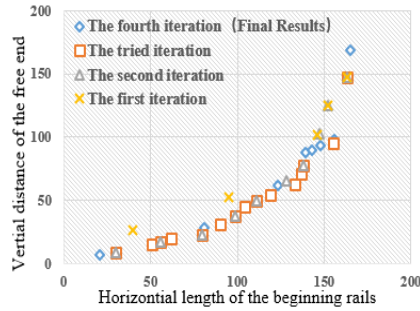


Fig 5 Optimal iterative process of middle guide

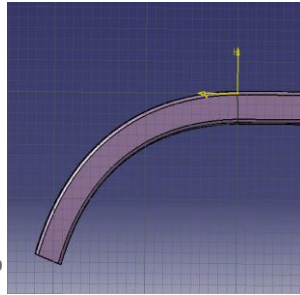


Fig 6 Model of bending part of middle guides

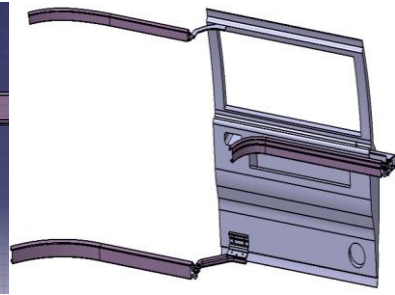


Fig 7 Sliding guide assembly drawing

The multi-objective iterative algorithm of trust region is adopted for the gray model. The quadratic iteration result is shown in Fig 5. As the iteration progresses, the resulting modular scatter gradually moves toward $\text{Min}\{f, F\}$, and the results comparison between the first iteration and the second iteration is obvious, and results between the fourth iteration and the third iteration do not change much, indicating that the results close to the convergence. The final-obtained 22 scatter-points are the vertical distance corresponding to the bending length of the corresponding rails, that is, the target scatter model which satisfies the force smoothing requirement, and the result is based on the model to draw the curved part of the guide (Fig.6).

This paper draws the upper, middle and lower rail models in CATIA, and shows the assembly diagram combined the rails with the wheels. Assembly diagram shown in Figure.7. The lower rail is indented by 80mm relative to the upper support arm in the horizontal direction, making the sliding door cambers by 4.1 degrees in the vertical direction. Under the gravity effect, guide wheel will attach to the rail, avoiding the gliding phenomenon.

3. Kinematic and kinetic performance determination of slide guide based on ADAMS

The simulation model of sliding guideway system is established in ADAMS, the 60N traction force is set in the center of gravity center of sliding gate, and the simulation data are used to judge the kinematics and dynamics of the system through the simulation data.

3.1 Kinematical performance determination

The sliding angle variation diagram (Fig 8) of the sliding gate with a precision of 0.05 seconds was obtained by the monitoring points MARKER_83 and MARKER_84 respectively. It is known that the slope angle of the whole sliding process is less than 0.5 degrees and there is no harmonic resonance curve. The change is very small for sliding door, so that the vibration stability of sliding door on sliding guide conforms to the requirement.

As Fig 9 shows that the acceleration is smoother before the roller enters the curved orbit. Compared with the slip gate velocity diagram in Fig 10, it can be found that the acceleration is fluctuating but less than $\pm 0.6 \text{ m/s}^2$. The motion velocity increases slightly, and the velocity curve is quite smooth in the whole movement process. The displacement is basically linear with the time of sliding doors when the doors slid on a linear guideway as shown in Fig 11. The increased volume of displacement gradually reduces in the curved guide, which is consistent with the actual situation. Therefore, the motion of the system is smooth and meets the requirements of smoothness.

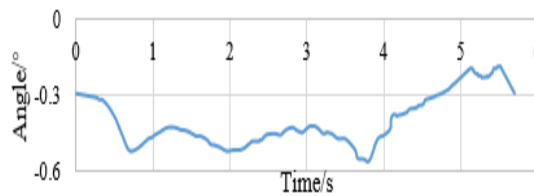


Fig 8 Changes in the tilt angle of sliding door

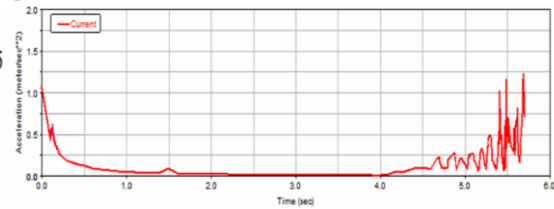


Fig 9 Acceleration of sliding gate diagram

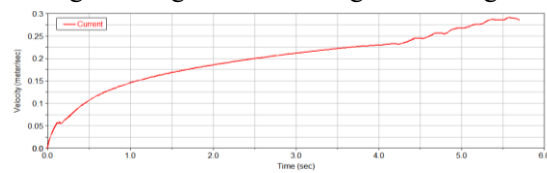


Fig 10 Velocity of sliding gate diagram

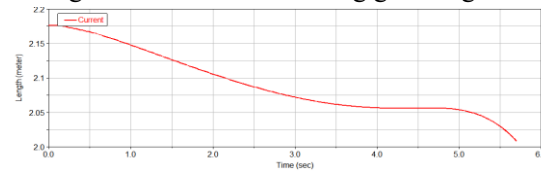


Fig 11 Time-displacement of sliding gate diagram

3.2 Determination of the dynamic performance

The dynamic performance of sliding guide is mainly embodied in the three-dimensional force of the combination of roller and guideway. The dynamic properties of each junction directly affect the dynamic mechanical properties of the whole system^[21]. The design of roller mechanism is intended to assume that the bearing wheel is bearing the plane force and is not under the vertical force. The bearing wheel bears the vertical force and is not subjected to the plane force.

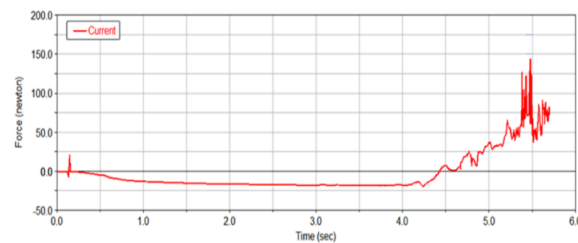


Fig 12 Force diagram for front guide pulley of lower rail in x direction

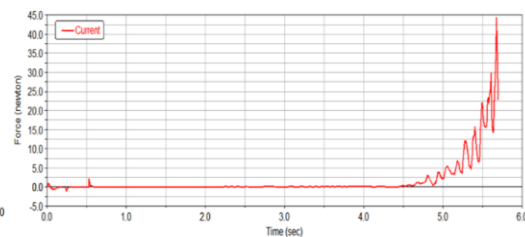


Fig 13 Force diagram for front guide pulley of lower rail in x direction

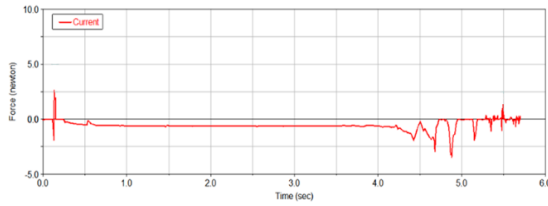


Fig 14 Force diagram for front guide pulley of lower rail in x direction

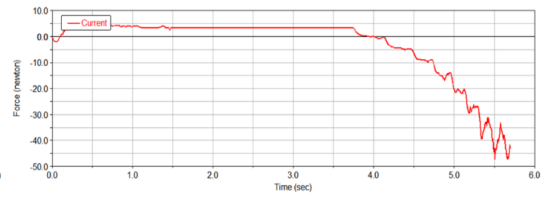


Fig 15 Force diagram for front guide pulley of lower rail in x direction

Take the rear and back guide pulley of the lower guide wheel for example. There is a slight vibration in the initial and final stages of the closed door by three-dimensional force which is showed in Fig.12, Fig.13 and Fig.14. In the linear stage of the sliding rail, the guide pulley is stressed uniformly in the x direction without vibration basically, scarcely in the y direction and about 1N in the vertical direction (z direction), which can be ignored. Through the comparison between the Figure 12 and Figure 15, it can be seen that the force-bearing of the front guide wheel in the x direction during the closing stage of the sliding door is far more than that of the rear guide wheel.

Take the middle bearing wheel for example. Before the roller mechanism enters the curved guide section, the bearing wheels suffer a slight concussion only at the initial stage in the form of x, y, z directions as shown in Fig 16, Fig 17 and Fig 18. After that, the linear guide part is very smooth, and the bearing wheels in the linear part of the rail does not bear the plane force but bear the gravity only in the vertical direction. In the bending part of the guide, the three-way force of the bearing wheel is oscillating, and the amplitude does not exceed $\pm 7\text{N}$ in the plane force. The amplitude in the vertical direction does not exceed $\pm 10\text{N}$, which is about 7.4% of the vertical force. Therefore, the requirements of ride comfort and ergonomics are satisfied.

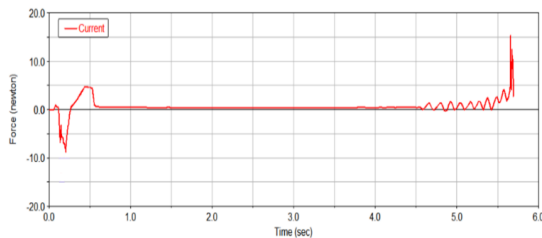


Fig 16 The x direction of force-bearing wheel of the middle guide diagram

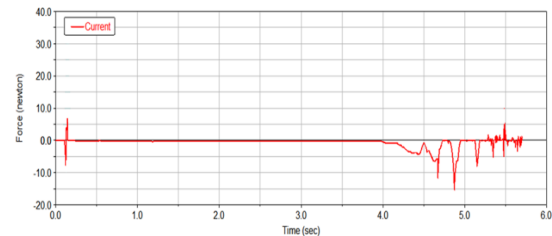


Fig 17 The y direction of force-bearing wheel of the middle guide diagram

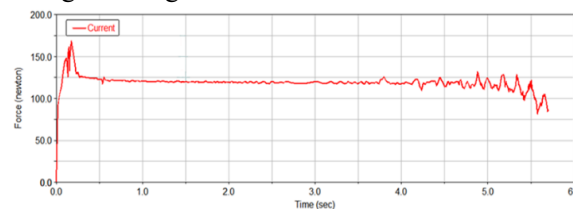


Fig 18 The z direction of force-bearing wheel of the middle guide diagram

4. Conclusion

Through the ADAMS simulation results, we know that the sliding guide wheel mechanism three-way force design and gray model trust region multi-objective optimization algorithm, can successfully solve the problem of mechanical design. In this paper, the multi-body dynamics complex mechanical system analysis method is used to study the three-way force and the smoothness of the sliding mechanism under the forced motion condition. The load characteristics

of the sliding guides with different design concepts are obtained. In order to realize the optimal cooperation motion of the components of the system and satisfy the NVH index and ergonomics performance, a stable sliding guide system based on the force of the carrier is proposed. A method of dealing with complex nonlinear engineering optimization problem is proposed by combining the trust region and multi-objective optimization by establishing the target model part by the gray model.

5. References

- [1] Chen Guodong, Han Xu. Multi-objective optimization method based on metamodel and its applications in vehicle body design [J]. *Journal of mechanical engineering*,2014(9).70
- [2] Chen Jianping, Yang Jiajun, Chen Yuanxiong, Zhao Meiling. Vibration analysis of roller linear guide's contact interface [J]. *Mechanical & Electrical Engineering Magazine*,2013, 30(3): 296– 299
- [3] Hasan Alipour, Mohammad Bagher Bana Sharifian, Hadi Afsharirad, A PID Sliding Mode Control for Ropeless Elevator Maglev Guiding System[J]. *Scientific Research-Energy and Power Engineering*, 2012,4,158-164
- [4] Guo Kejian, Li Hongguang, Meng Guang. Modeling and Simulation of Vibration for Slide Guide System in an Elevator [J]. *Journal of Vibration and Shock*, 2008, (10):39-42
- [5] Fan Qingshan, et al *Theoretical Mechanics* (Tsinghua University edition), Higher Education Press.2000,2.
- [6] Chen Guodong, Bu Zhuzhou. A Multi-Objective Optimization Scheme and Its Application Based on Sequential Radial Basis Function. *Automotive Engineering*,2015,37(9):1077-1083
- [7] Tan Jinpeng. Study on the Method for Dynamic Optimum Design of Structures Based on Trust Region Method (Master's Graduation Thesis). Beijing: Tsinghua University,2006
- [8] Ou Yigui. A Survey of Trust Region Methods for Solving Nonlinear Optimization Problems. *Journal of Hainan University*,2003,21(3):272-277
- [9] Yuan Yaxiang, Sun Wenyu. *Optimization Theory and method*. Beijing: Science Press,1997
- [10] Qiu Z P.Comparison of Static Response of Structures Using Convex Models and Interval Analysis Method[J].*International Journal for Numerical Methods in Engineering*, 2003,56:1735-1753.
- [11] Qiu Zhiping. *Convex Method Based on Non-probabilistic set-theory and its application*[M]. Beijing: National Defense Industry Press.2005.
- [12] Abbas M.Bellahcene F.Cutting Plane Method for Multiple Objective Stochastic Integer Linear Programming[J].*European Journal of Operational Research*,2006,168(3):967-984.
- [13] Liu B D,Iwamura K.Fuzzy Programming with Fuzzy Simulation-based Genetic Algorithm[J]. *Fuzzy Sets and Systems*.2001.122:253-262.
- [14] Khokhar Z O,Vahabzadeh H,Ziai A,et al.On the performance of the psp method for mixed-variable multi-objective design optimization. *Journal of Mechanical Design*,2010,132(7): 1-11
- [15] Kurtaran H,Eskandarian A,Marzougui D,et al.Crashworthiness design optimization using successive response surface approximations. *Computational Mechanics*,2002,29(4):409-421
- [16] Jiang C,Han X,Liu G P.A sequential nonlinear interval number programming method for uncertain structures. *Computer Methods in Applied Mechanics and Engineering*,2008,197(49-50): 4250-4265
- [17] Liu G P,Han X,Jiang C.A novel multi-objective optimization method based on an approximation model management technique. *Computer Methods in Applied Mechanics and Engineering*, 2008,197(33-40):2719-2731

- [18] Sun Chengzhi, Chen Guanlong, Li Shuhui, Lin Zhongqin. The effect of variable blank-holder forces on formability of ractangle box deep drawing [J]. Journal of Plasticity Engineering, 2003(10): 6-9
- [19] Li Xinlan, Jiang Chao, Han Xu. AnUncertainty Multi-objetive Optimization Based on Interval Analysis and Its Application [J]. China Mechanical Engineering, 2011(9):1100-1106
- [20] Chen Guodong, Han Xu,Liu Guiping. A multi-objective optimization method based on approximate model management[J]. Engineering Mechanics,2010(5):205-209
- [21] Guo Chenglong, Yuan Juntang, Wang Weiyou, Xia Lingling, Huang Jun. Experimental Research on Dynamic Stiffness of Sliding Guide's Joints. China Mechanical Engineering, 2012, 23(9):1021-1025